Available online at www.sciencedirect.com
ScienceDirect
Trans. Nonferrous Met. Soc. China 23(2013) 3242−3248
Transactions of Nonferrous Metals Society of China
www.tnmsc.cn

# Overflowing phenomenon during ultrasonic treatment in Al−Si alloys

Yu-bo ZHANG, Yi-ping LU, Jin-chuan JIE, Ying FU, De-shui ZHONG, Ting-ju LI

School of Material Science and Engineering, Dalian University of Technology, Dalian 116024, China

Received 19 December 2012; accepted 13 April 2013

**Abstract:** At the late stage of solidification with ultrasonic treatment (UST) in Al−Si alloys, a part of semisolid overflows and climbs along the probe. The interesting phenomenon and its influence on the solidification microstructure were investigated in order to better study the mechanism of UST. It is considered that the overflowing phenomenon occurs due to the changes of vibration and flow in the remaining semisolid. Because the overflowed portion comes from the region with intense UST effect and vibrates with the probe during solidification, great modification of primary and eutectic Si (about 10 μm in length) and refinement of primary $\alpha$(Al) (about 70 μm in size) are observed in this portion.

**Key words:** Al−Si alloy; ultrasonic treatment; overflowing phenomenon; solidification microstructure

## 1 Introduction

Al−Si alloys are widely used in the fields of automotive manufacture, aerospace and military research due to their low density, high specific strength, and good wear resistance. However, in normal casting, there are acicular eutectic Si and large primary Si which are greatly disadvantageous to mechanical properties of Al−Si alloys. In addition, fine grains are generally beneficial to enhancing the mechanical properties. Therefore, it is important to improve grain refinement and modification of Si phase during material processing.

Addition of chemical elements [1,2] is a favorable method to modify the primary and eutectic Si. Some other methods are also used to refine the microstructure during the metal solidification process, for instance, electromagnetic stirring [3], intensive shearing [4], addition of grain refiner [5] and ultrasonic vibration [6−11]. Among these methods, ultrasonic treatment (UST) has attracted great interest in the last twenty years due to its evident effect on grain refinement. At present, different mechanisms may be responsible for the modification of microstructure caused by UST, which are summed up in three main points: 1) the improvement of heterogeneous nucleation; 2) the promotion of cavitation-induced nucleation; 3) the fragmentation of growing dendrites. The cavitation is considered to be the most important phenomenon when the power ultrasound is applied to liquid. It is the formation, growth and then immediate implosion of the cavitation bubbles in liquid. It can clean the surface of insoluble inclusions including oxides and impurities, and improve their wettability with the melt, resulting in the enhancement of heterogeneous nucleation [12]. When the cavitation bubbles implode, it causes great fluctuation of pressure and reversal of boundary velocity. On the one hand, the sharp increase of localized pressure is useful to the promotion of undercooling homogeneous nucleation, by increasing the melting point based on the Clausius-Clapeyron equation [13]. On the other hand, the implosion of bubbles brings about a strong shock wave, causing the fragmentation of the single crystals [14], secondary arms and even the primary trunk [15].

The refinement mechanism of UST during metal solidification has been preliminarily established, and some particular phenomena of ultrasound are still under research. It is necessary to further study the ultrasonic effect to provide experimental and theoretical basis for its widely industrial usage. For this reason, more attention should be paid to the special phenomena of UST. In this work, an interesting phenomenon named overflowing phenomenon is studied for the first time, its effect on microstructure evolution is investigated as well.

**Foundation item:** Project (50874022) supported by the National Natural Science Foundation of China
**Corresponding author:** Ting-ju LI; Tel/Fax: +86-411-84708940; E-mail: tjuli@dlut.edu.cn
DOI: 10.1016/S1003-6326(13)62859-9

## 2 Experimental

Commercial pure Al and Si were used to prepare the Al−Si alloys, which are hypereutectic alloy A, near-eutectic alloy B and hypoeutectic alloy C, as listed in Table 1. Different experiment parameters correspond to each composition Al−Si alloy.

**Table 1** Chemical compositions of Al−Si alloys used in this work (mass fraction, %)

| Alloy | Si | Fe | Al |
|---|---|---|---|
| A | 17.8 | 0.1 | Bal. |
| B | 11.6 | 0.1 | Bal. |
| C | 6.7 | 0.1 | Bal. |

For alloy A, it was melted and kept at 750 °C in an electric resistance furnace. Then the melt was transferred into a preheated (at 750 °C) cylindrical graphite crucible, with the internal diameter of 60 mm and height of 80 mm. The crucible was placed on an insulation board and cooled in the air. The original sample A−1 was prepared without UST. When the temperature reached 708 °C (50 °C higher than the liquidus temperature), power ultrasound was applied with the probe (30 mm in diameter) inserting to a depth of 10 mm under the melt surface. The frequency and power of ultrasound were 20 kHz and 260 W, respectively. After UST for about 120 s, the overflowing phenomenon began, while the temperature of the semisolid near the probe was 625 °C. The overflowing phenomenon would last until the ingot was solidified. The overflowing object was shown in Fig. 1, which was taken down and prepared as sample A−3. For comparison with the effect of normal UST, sample A−2 was prepared from the remaining ingot, which was located 20 mm below the top surface of ingot.

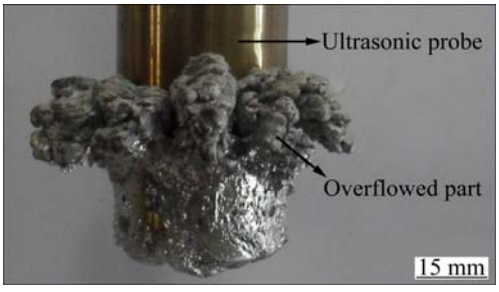


**Fig. 1** Overflowed object obtained in this work

In order to clarify the influence of cooling condition on the microstructure evolution of the overflowed portion, a sample was prepared by fast solidification to compare with the overflowed portion. This sample was solidified in a water-cooling copper mould, which is obconical, 25 mm in length and 10 mm in diameter. The cooling rates under different conditions are listed in Table 2.

**Table 2** Cooling rates under different conditions

| Cooling rate | Value/(°C·s$^{-1}$) |
|---|---|
| Normal solidification (in the air) | 1 |
| Overflowed portion | 2−3 |
| In copper mould | 30−50 |

Other two experiments of Alloys B and C were carried out under the same experimental conditions. The detailed experimental parameters are listed in Table 3.

All the samples were ground and polished mechanically to observe the microstructure by optical microscopy. The morphology evolution of eutectic Si was observed by scanning electronic microscopy (SEM) after deep etching.

**Table 3** Experimental parameters of UST and overflowing phenomenon

| Alloy | Ultrasonic treatment temperature/°C | Liquidus temperature/ °C | Initial temperature of overflowing phenomenon/°C |
|---|---|---|---|
| A | 708 | 658 | 625 |
| B | 634 | 584 | 580 |
| C | 667 | 617 | 608 |

## 3 Results

Figure 2 shows the microstructures of Al−Si alloys under different conditions. Without UST, the microstructure of Alloy A consists of primary Si and eutectic structure (Fig. 2($a_1$)). The average length of primary Si is more than 60 μm. By contrast, most primary Si becomes smaller and more compact under UST (Fig. 2($a_2$)). However, the acicular eutectic Si has no obvious changes in appearance. In the overflowed portion (Fig. 2($a_3$)), the remarkable morphological modification of primary and eutectic Si can be observed. The coarse primary Si and acicular eutectic Si are substituted by fine granular Si, with the average length of 8 μm. It is difficult to distinguish the primary and eutectic Si because the difference is not obvious. The quantitative element analysis by EPMA proves that the particles observed in overflowed portion are mainly Si, rather than intermetallics or inclusions.

The microstructure evolution of Alloy B is similar to that of Alloy A. The original microstructure without UST consists of developed dendritic primary $\alpha$(Al) and eutectic structure (Fig. 2($b_1$)). When the alloy was treated by ultrasound, the developed dendrite is substituted by equiaxed $\alpha$(Al), and some modified Si can be observed in the interdendritic region (Fig. 2($b_2$)). The result is in accordance with the previous work [16]. In the

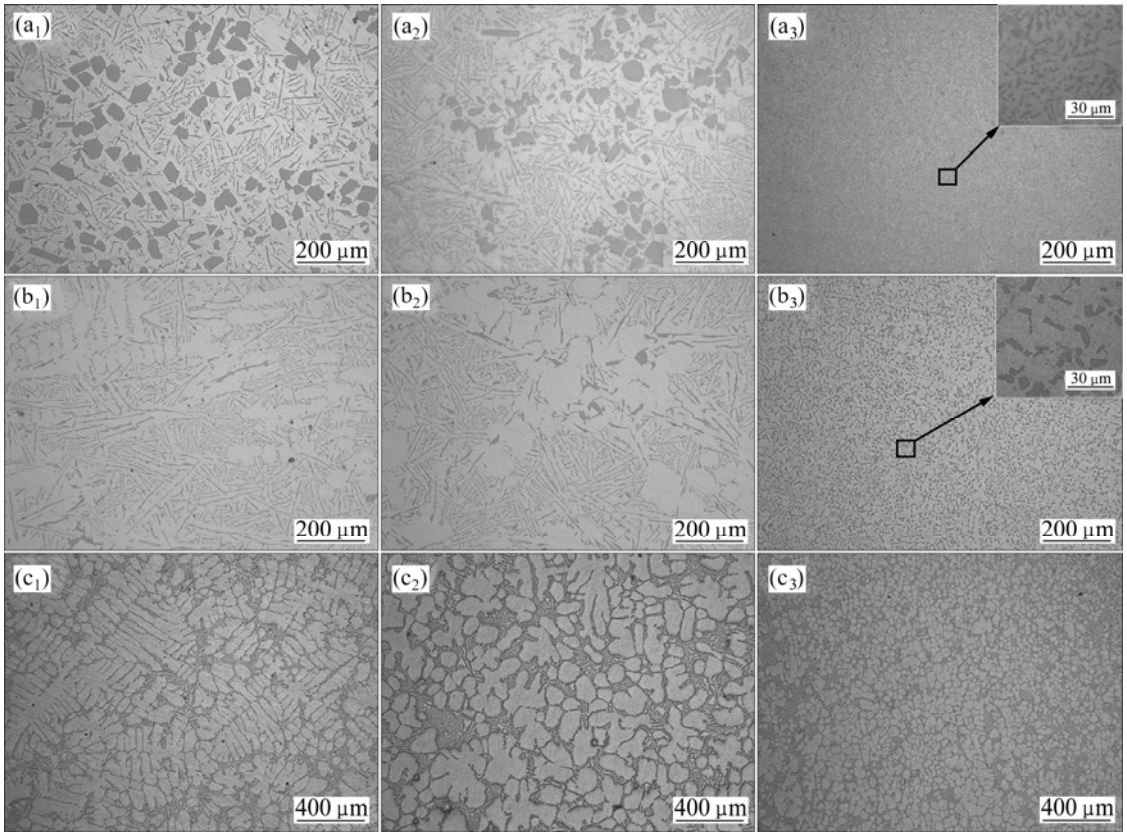


**Fig. 2** Microstructures of different Al−Si alloys under different conditions: ($a_1$) Unmodified Alloy A; ($a_2$) Alloy A with UST; ($a_3$) Overflowed Alloy A; ($b_1$) Unmodified Alloy B; ($b_2$) Alloy B with UST; ($b_3$) Overflowed Alloy B; ($c_1$) Unmodified Alloy C; ($c_2$) Alloy C with UST; ($c_3$) Overflowed Alloy C

overflowed portion, the morphology of eutectic Si changes from acicular to granular shape (Fig. 2($b_3$)). The average length of eutectic Si reduces from 90 μm to 10 μm. Figure 3 shows the three-dimensional morphology evolution of eutectic Si observed by SEM. The result indicates that normal UST fails to modify the morphology of eutectic Si (Fig. 3(b)), which is still coarse and plate-like. However, eutectic Si in the overflowed portion is modified to fine and granular (Fig. 3(c)). Figure 4 shows the results of quantitative metallographic analysis of Si morphology. The comparisons of the average size and the aspect ratio suggest that the primary and eutectic Si in the overflowed portion are highly modified.

The microstructure evolution of hypoeutectic Alloy C is shown in Figs. 2($c_1$), ($c_2$) and ($c_3$). The size of primary $\alpha$(Al) is reduced by the application of UST, but the decrease of size is more obvious in the overflowed portion. Moreover, the primary $\alpha$(Al) in the overflowed portion is globular, rather than dendritic.

In this experiment, UST can reduce the grain size of $\alpha$(Al) but fails to form a better morphology of primary and eutectic Si (Figs. 2($a_2$) and ($b_2$)). As reported in Refs. [6,17−19], the researchers did not obtain the same experimental results of fine Si with UST. The mechanism of UST on the modification of eutectic Si is not clear at present. It is considered that due to the low heat release in the effective region of UST, some nuclei have enough time to grow up to blocky Si rather than acicular eutectic Si, which lies in the interdendritic region of $\alpha$(Al) (Fig. 2($b_2$)). For another case, the growth of acicular eutectic Si may be suppressed by the refinement of primary $\alpha$(Al). By contrast, the microstructure of the overflowed portion is quite different, especially for the morphology of primary and eutectic Si. There should be another mechanism for the microstructure evolution in the overflowed portion, which is different from of normal UST.

## 4 Discussion

### 4.1 Factors for overflowing phenomenon

The overflowing phenomenon occurs at the late stage of solidification process. The changes of flow and vibration in the remaining semisolid are responsible for the overflowing behaviour.

In recent studies, most researchers use power ultrasound by inserting the probe vertically into the melt, because ultrasonic energy transmits into the melt with lower loss in this way. It is now widely accepted that this

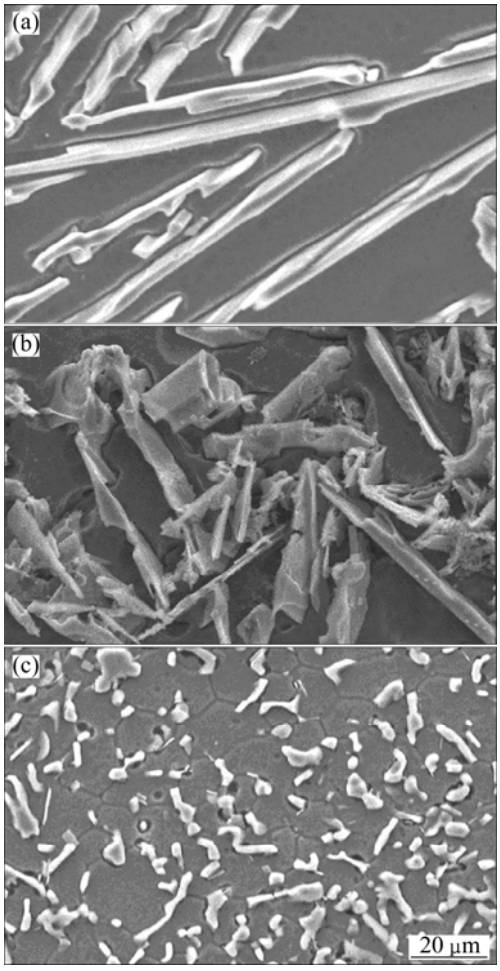


**Fig. 3** Morphologies of eutectic Si: (a) Unmodified; (b) With UST; (c) Overflowed

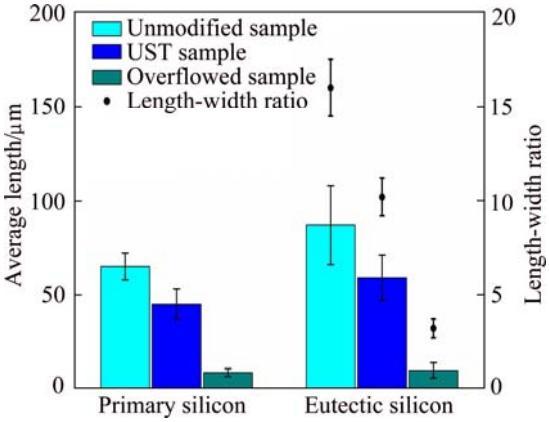


**Fig. 4** Morphological analyses of primary and eutectic Si under different conditions

application manner of power ultrasound generates symmetric circulations (the acoustic streaming) in liquid, which is conducive to uniform distribution of the temperature and concentration [17,20]. BRADLEY [21] indicated that the ultrasonic probe has a big influence on driving flow. The boundary condition, especially at the surface of ultrasonic probe, determines the flow-driving mechanism. At the late stage of solidification, the solidification front moves close to the ultrasonic probe, resulting in the change of the boundary condition. It is reasonable that the fluid motion will change due to the diminishing semisolid (the temperature of the remaining is lower than the liquidus temperature). The acoustic streaming probably transforms from solenoidal to irrotational current under this circumstance. In other words, when the current rushes to the solidification front, it will flow back to the annular gap surrounding the probe. The flow should be related to the spilling of semisolid.

In addition, when the solidification front nearly contacts the probe, the radial oscillatory flow in annular gap $j$ (surrounding the probe) can be easily established to have an amplitude $A'$ [20]

$$A' = (R/2j)A_0 \quad (1)$$

where $R$ is the radius of the probe; $j$ is the width of annular gap between the probe and the solidification front; $A_0$ is the amplitude of the transducer. It is evident that the remaining semisolid in the annular gap will have a large amplitude, when $j$ is smaller than $R$. On one hand, this strong vibration may be the most efficient in generating an oscillatory flow to break the growing dendrite mesh, causing grain refinement in this part [20]. On the other hand, the magnifying amplitude provides another force to put the semisolid up.

### 4.2 Microstructure evolution in the overflowed portion

As shown in Fig. 2, the microstructure in the overflowed position is greatly refined, more importantly, the primary and eutectic Si are modified to particles in this position. The effect of refinement in the overflowed position is more remarkable than that with normal UST. The fast cooling rate, intense ultrasonic impact and vibration during solidification may be responsible for the microstructure evolution in the overflowed position.

As shown in Table 2, the overflowing is solidified faster than the remaining semisolid in the graphite crucible. It is well known that fast solidification can refine $\alpha$-Al and suppress the growth of eutectic Si. In order to clarify the effects of fast cooling on the microstructure modification of the overflowed portion, some samples were prepared in a water-cooling copper mould, the cooling rate of which (30−50 °C/s) is higher than that of the overflowed portion (2−3 °C/s). Figure 5 shows the microstructures of the samples prepared by the copper mould. The microstructure is refined due to the suppression of growth process by fast solidification, including primary Si, $\alpha$(Al) and eutectic Si. However, the primary and eutectic Si obtained by fast solidification are

still blocky and acicular (Figs. 5(a) and (b)) in appearance, respectively. By contrast, the microstructures of the overflowed portion are quite different from those of copper mould solidification. Although it is difficult to distinguish the primary and eutectic Si in the hypereutectic Alloy A (Fig. 2($a_3$)), the granular Si is much smaller than the blocky primary Si of fast solidification (Fig. 5(a)). In addition, primary $\alpha$(Al) of Alloy C in the overflowed portion is globular (Fig. 2($c_3$)) instead of developed dendritic structure of fast solidification (Fig. 5(c)).

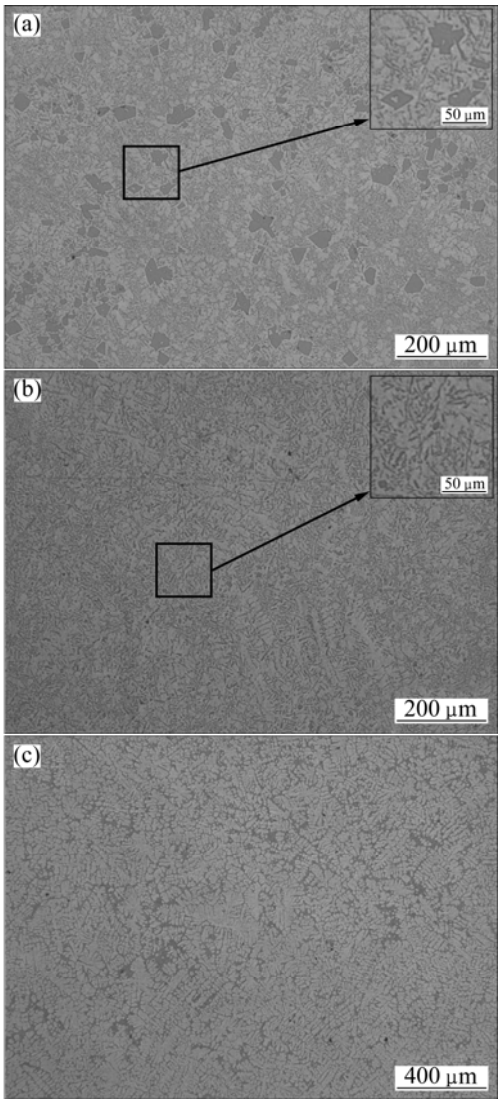


**Fig. 5** Microstructures of copper mould solidified samples: (a) Alloy A; (b) Alloy B; (c) Alloy C

Consequently, it is considered that fast solidification can refine the microstructure effectively, but it is not the primary cause for the great modification of Si in the overflowed portion. Intense ultrasonic impact and strong vibration during solidification are the reasons for the microstructure evolution in the overflowed portion.

For normal UST, the ultrasonic intensity and amplitude will greatly decrease with increasing ultrasonic propagation distance in the metal melt. Energy loss is the reason for the ultrasonic attenuation, which includes beam spread, diffraction, acoustic scattering and energy transformation from acoustic to heat. The displacement $A$ and the intensity $I$ in liquid will attenuate with the propagation distance $x$, according to the equations as follows [22]:

$$A = A_0 e^{-\alpha x} \tag{2}$$

$$I = I_0 e^{-\alpha x} \tag{3}$$

where $A_0$ and $I_0$ are the amplitude and intensity of the transducer, respectively; $x$ is the distance from the undersurface of the probe; $\alpha$ is the attenuation coefficient which is related to the ultrasonic frequency and medium properties. It is accepted that the vibration and acoustic pressure of melt will weaken along the ultrasonic propagation path [15]. Similarly, the effect of UST on refining the microstructure will decline with increasing distance from the probe. In this experiment, a gradual refinement as a function of distance from the undersurface of probe can be observed. Figure 6 shows the microstructures of hypoeutectic Alloy C at distances of 3 mm, 30 mm, and 60 mm from the undersurface of the probe which were obtained in this experiment. The gradual morphological change of primary $\alpha$(Al) proves that the effect of UST on refinement declines with increasing distance from the probe.

By contrast, the overflowed portion comes from the region hardly with ultrasonic attenuation. The overflowing is from the last solidified region, which is regarded as the area with the most intense ultrasonic effect. The overflowed portion will contain the primary phase and near-eutectic melt with a large number of cavitation-induced nuclei. Most nuclei will be retained during solidification and overflowed process, resulting in the microstructure modification.

After spilling and climbing up, the overflowed semisolid vibrates with the probe during solidification. It vibrates with high frequency and large amplitude equal to the ultrasonic transducer, which is stronger than the remaining semisolid in the crucible. The strong vibration can break the growing dendrite and restrict the growth of primary and eutectic Si. Hence, under the collective effect of intense UST and strong vibration, great modification of primary and eutectic Si and refinement of globular primary $\alpha$(Al) are observed in the overflowed portion.

In addition, the experiments have been carried out for many times and the overflowing phenomenon can be observed each time. Because of the great refinement in overflowed potion, it will be significant if this phenomenon can be realized in industrial research or production. Thus, based on the overflowing phenomenon,

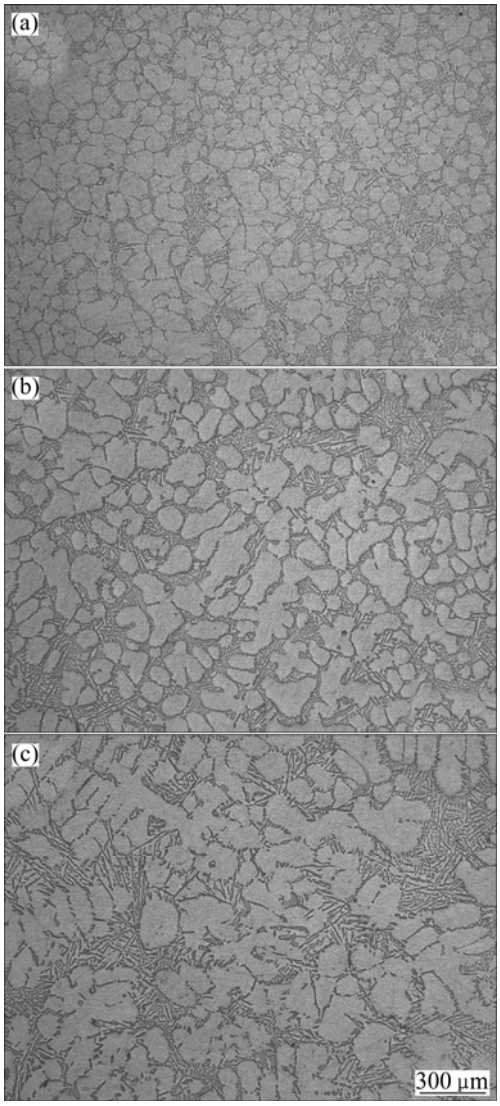


**Fig. 6** Microstructures of ingot under UST at distances of 3 mm (a), 30 mm (b) and 60 mm (c) from undersurface of probe

further work concerning the grain refinement and microstructural modification in the semisolid process of Al−Si alloy is now in processing.

## 5 Conclusions

The overflowing phenomenon during UST in Al−Si alloys is beneficial to the microstructure modification. This is more obvious than the influence of normal UST. Due to the intense ultrasonic treatment and strong vibration during solidification, highly modified Si and refined $\alpha$(Al) are observed in the overflowed portion. The primary and eutectic Si in the overflowed portion is modified to granular shape. The average length of primary and eutectic Si reduces from 60 to 8 μm and from 90 to 10 μm, respectively. The primary $\alpha$(Al) is greatly refined to globular shape with the size of 70 μm. Due to the remarkable effect on the microstructure modification of Al−Si alloys, further research is needed to achieve a complete understanding of the overflowing phenomenon and its industrial applications.

## References

[1] LIU Yuan, DING Chao, LI Yan-xiang. Grain refining mechanism of Al−3B master alloy on hypoeutectic Al−Si alloys [J]. Transaction of Nonferrous Metals Society of China, 2011, 21: 1435−1440.

[2] NOGITA K, McDONALD S D, DAHLE A K. Eutectic modification of Al−Si alloys with rare earth metals [J]. Mater Trans, 2004, 45: 323−326.

[3] CUI Jian-zhong, ZHANG Zhi-qiang, LE Qi-chi. DC casting of light alloys under magnetic field [J]. Transaction of Nonferrous Metals Society of China, 2010, 20: 2046−2050.

[4] KOTADIA H R, HARI BABU N, ZHANG H, FAN Z. Microstructural refinement of Al−10.2%Si alloy by intensive shearing [J]. Mater Lett, 2010, 64: 671−673.

[5] WANG Tong-min, CHEN Zong-ning, FU Hong-wang, XU Jun, FU Ying, LI Ting-Ju. Grain refining potency of Al−B master alloy on pure aluminum [J]. Scripta Mater, 2011, 64: 1121−1124.

[6] JIAN X, MEEK T T, HAN Q Y. Refinement of eutectic Si phase of aluminum A356 alloy using high-intensity ultrasonic vibration [J]. Scripta Mater, 2006, 54: 893−896.

[7] ABRAMOV O V. Action of high intensity ultrasound on solidifying metal [J]. Ultrasonics, 1987, 25: 73−82.

[8] ESKIN G I. Influence of cavitation treatment of melts on the processes of nucleation and growth of crystals during solidification of ingots and casting from light alloys [J]. Ultrason Sonochem, 1994, 1: s59−s63.

[9] MAO Da-heng, ZHANG Yun-fang, NIE Zhao-hui, LIU Q, ZHONG Jue. Effects of ultrasonic treatment on structure of roll casting aluminum strip [J]. Journal of Central South University of Technology, 2007, 14: 363−369.

[10] ZHANG Li-hua, YU Jun, ZHANG Xiao-ming. Effect of ultrasonic power and casting speed on solidification structure of 7050 aluminum alloy ingot in ultrasonic field [J]. Journal of Central South University of Technology, 2010, 17: 431−436.

[11] WU Shu-sen, ZHONG Gu, WAN Li, AN Ping, MAO You-wu. Microstructure and properties of rheo-diecast Al−20Si−2Cu−1Ni−0.4Mg alloy with direct ultrasonic vibration process [J]. Transaction of Nonferrous Metals Society of China, 2010, 20: s763−s767.

[12] KHOSRO AGHAYANI M, NIROUMAND B. Effects of ultrasonic treatment on microstructure and tensile strength of AZ91 magnesium alloy [J]. J Alloys Compd, 2011, 509: 114−122.

[13] RAMIREZ A, QIAN M, DAVIES B, WILKS T, STJOHN D H. Potency of high-intensity ultrasonic treatment for grain refinement of magnesium alloys [J]. Scipta Mater, 2008, 59: 19−22.

[14] WAGTERVELD R M, BOELS L, MAYER M J, WITKAMP G J. Visualization of acoustic cavitation effects on suspended calcite crystals [J]. Ultrason Sonochem, 2011, 18: 216−225.

[15] SHU D, SUN B D, MI J W, GRANT P S. A high-speed imaging and modeling study of dendrite fragmentation caused by ultrasonic cavitation [J]. Metall Mater Trans A, 2012, 43: 3755−3766.

[16] DAS A, KOTADIA H R. Effect of high-intensity ultrasonic irradiation on the modification of solidification microstructure in a Si-rich hypoeutectic Al−Si alloy [J]. Mater Chem Phys, 2011, 125: 853−859.

[17] JIAN X, XU H, MEEK T T, HAN Q Y. Effect of power ultrasound on solidification of aluminum A356 alloy [J]. Mater Lett, 2005, 59: 190−193.

[18] KOCATEPE K, BURDETT C F. Effect of low frequency vibration on macro and microstructure of LM6 alloys [J]. J Mater Sci, 2000, 35: 3327−3335.

[19] NAFISI S, EMADI D, SHEHATA M T, GHOMASHCHI R. Effects of electromagnetic stirring and superheat on the microstructural characteristics of Al−Si−Fe alloy [J]. Mater Sci Eng A, 2006, 432: 71−83.

[20] CAMPBELL J. Effects of vibration during solidification [J]. Int Met Rev, 1981, 2: 71−102.

[21] BRADLEY C E. Acoustic streaming field structure: The influence of the radiator [J]. J Acoust Soc Am, 1996, 100: 1399−1408.

[22] PUGA H, TEIXEIRA J C, BARBOCA J, SEABRA E, RIBEIRO S, PROKIC M. The combined effect of melt stirring and ultrasonic agitation on the degassing efficiency of $AlSi_9Cu_3$ alloy [J]. Mater Lett, 2009, 63: 2089−2092.

# 超声处理铝硅合金过程中的溢出现象

张宇博，卢一平，接金川，傅 莹，钟德水，李廷举

大连理工大学 材料科学与工程学院，大连 116024

**摘 要**：在超声处理铝硅合金的过程中，伴随着金属液的凝固，一部分半固态金属会在超声工具头附近溢出并沿工具头向上爬升。研究超声处理过程中的这种特殊现象，并对其成因及溢出部分的微观组织变化进行讨论。结果表明：溢出现象与半固态金属中的液体流动和振动模式变化有关。溢出部分来自于超声作用最强烈的区域，且在凝固过程中随超声工具头进行高频振动，因此在溢出部分得到十分细化的凝固组织。初生 $\alpha$(Al)由粗大的树枝晶变为细小的等轴晶，尺寸减小为约 70 μm；块状初生硅和针片状共晶硅全部变为细小的硅晶粒，尺寸减小至约 10 μm。

**关键词**：铝硅合金；功率超声；溢出现象；凝固组织

**(Edited by Chao WANG)**